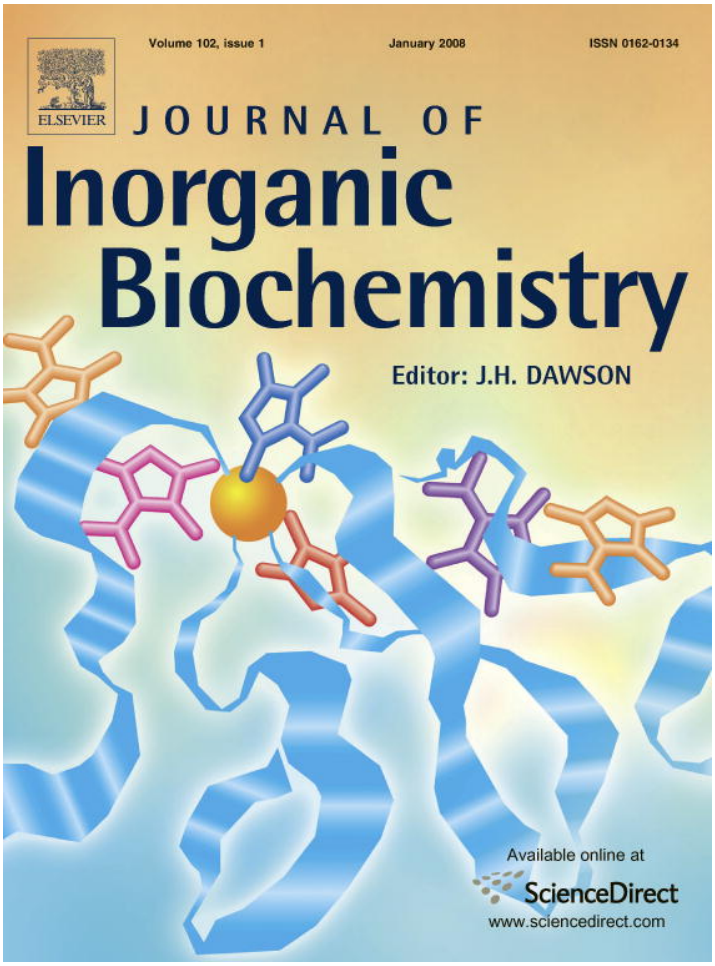

Available online at www.sciencedirect.com
ScienceDirect
Journal of Inorganic Biochemistry 102 (2008) 53–62
Journal of Inorganic Biochemistry
www.elsevier.com/locate/jinorgbio

A computational study on DNA bases interactions with dinuclear tetraacetato-diaqua-dirhodium(II,II) complex

Jaroslav V. Burda [a,*], Jiande Gu [b]

[a] Department of Chemical Physics and Optics, Faculty of Mathematics and Physics, Charles University, Ke Karlovu 3, 121 16 Prague 2, Czech Republic
[b] Center for Drug Discovery and Design and State Key Laboratory of Drug Research, Shanghai Institute of Materia Medica, Shanghai Institutes for Biological Sciences, Chinese Academy of Sciences, 294 Taiyuan Road, Shanghai 200031, PR China

Received 3 April 2007; received in revised form 22 June 2007; accepted 26 June 2007
Available online 7 July 2007

Abstract

In our study, we have determined the thermodynamic behavior for the replacement reaction of one and two acetyl-ligands from the diaqua-tetrakis(μ-acetylato)dirhodium(II,II) complex by purine DNA bases. The complexes were optimized at the density functional theory (DFT) level with the B3LYP functional. Stuttgart–Dresden pseudopotentials were used for the description of the Rh atoms. Most of the replacement reactions are mildly exothermic, ΔG is up to 12 kcal/mol for the first acetyl-ligand and up to 8 kcal/mol for the second ligand replacement. For all explored complexes, stabilization and bonding energies were computed together with selected electronic properties. Adenine base coordinates to the dirhodium complex slightly more firmly than guanine. In head-to-tail conformation the two guanines are better stabilized (by about 8 kcal/mol) than in head-to-head arrangement due to minimization of sterical repulsion of both bases. We have shown that the bonding energy of axial water ligands is very small (up to 13 kcal/mol), resembling more H-bonds than dative coordination. Despite the larger stabilization energies of adenine-containing complexes, the thermodynamic parameters of the studied replacement reactions are more favorable in case of guanine complexes. Higher exothermicity is connected with easier deprotonization of guanine N1-site in comparison with N6-site of adenine in accord with experimental data.

Keywords: Quantum chemical calculations; Dirhodium complexes; Reaction thermodynamics; DNA interactions

1. Introduction

Since the early 60s when anticancer activity of cisplatin became known [1], many other transition metal complexes were probed as antitumor drugs, too. Especially due to the very high toxicity of cisplatin it is worth to study other substances in parallel to the development of cisplatin analogues. It is known that metallocene complexes of the Ti, Mo or V atoms can be used for this purpose, see, e.g., the review of Kuo et al. [2] where basic properties and activities are summarized. Some other recent works on the topic of metallocenes can be found in studies [3–7]. Titanocene dichloride has recently successfully passed the first phase of clinical tests. Also, the activity of Ru(III) complexes has been thoroughly studied [8–11]. The first phase of clinical trials has been recently passed by *trans*-$Cl_4(Me_2SO)(Im)Ru(III)$ (Im = imidazole) (cf. Formula 1).

Also the Ru(II) compounds – the so-called piano-stool complexes – have been recognized as very potent anticancer agents [12–15]. Dirhodium(II) complexes have been discovered as possible candidates for anticancer treatment, too. Their antitumor properties were noticed already in the 90s, as can be noticed in several studies [16–19]. An excellent review on rhodium anticancer activity was written by Katsaros and Anagnostopoulou [20], where not only Rh(II) but also other rhodium complexes were addressed. In this work, considerations on the length of carboxyl ligands are presented as well as possible interactions with

* Corresponding author. Fax: +420 221 911 249.
E-mail address: burda@karlov.mff.cuni.cz (J.V. Burda).

0162-0134/$ - see front matter © 2007 Elsevier Inc. All rights reserved.
doi:10.1016/j.jinorgbio.2007.06.041

some amino acids in proteins and peptides. Since the very beginning of the anticancer investigations of the dirhodium(II) compounds, the research group of Chifotides and Dunbar has been very active. They have performed many physico-chemical characterizations, especially an NMR structural exploration of metal adducts with diguanine or d(GpG) sequences [21,22] and a mass-spectroscopy study on binding properties [23]. In the latter study, the kinetic aspects of the metal addition were also examined. The obtained results were compared with the properties of the platinum complexes (cisplatin and carboplatin). The paper also suggests a probable molecular mechanism for the DNA base interactions with tetracarboxylate complexes $Rh_2(\mu\text{-}O_2CR)_4$. Moreover, measurements of variable oligomeric sequences where two adenine, adenine–guanine, and two guanine bases interact with a dirhodium complex were done, too. Comparable rates for the replacement of the acetyl group were observed in the case of coordination of the same bases (AA and GG). Slightly slower reaction rates were found for the formation of mixed AG and GA adducts. Their recent publications [24,25] present some deeper insights into the reaction mechanism and the role of various ligands in the formation of complexes active in antitumor processes.

In our study, the energy relations of the acetyl ligand(s) replacement with purine DNA base(s) are explored. Although adenine has not been used in experimental measurements, we have used it in model interactions of paddle-wheel dirhodium complex with poly/oligo-nucleotides, which were reported, e.g., in Refs. [23,25].

Since these dinuclear complexes have relatively complicated electronic structures, only the gas phase calculations were performed at this first stage. The influence of solvation effects and an exploration of possible reaction mechanisms (with a kinetic description of the reaction) are under investigation.

2. Computational details

The optimization of the selected structures was performed using the DFT technique with the B3PW91 functional and 6-31G(d) basis set. For the description of the Rh atoms, the Stuttgart–Dresden pseudopotentials were used [26]. The appropriateness of this description was tested with respect to all-electron calculations using the 3-21G(f) (the exponent of the *f* functions was taken from our optimization at the coupled clusters (CCSD) level on the atomic ground state $\alpha = 0.975$) and well-tempered Huzinaga's basis set [27,28] on the smallest tetraacetylato-dirhodium complex, comparing the eigenvectors and eigenvalues of the chosen basis sets. A correct electronic description is represented by the highest occupied molecular orbital (HOMO) composed from a sigma antibonding combination of Rh atomic orbitals (AOs) and the lowest unoccupied molecular orbital (LUMO) composed from a delta antibonding combination of Rh AOs (cf. the discussion of MOs below). Also a reasonable agreement of the dinuclear distance of 2.386 Å with the experimental value was obtained. The final energy analyses (reaction, stabilization, and bonding energies) were determined at the B3LYP/6-31++G(d,p) level of DFT. Stabilization energies and bonding energies (BE) were estimated in the framework of the basis set superposition error (BSSE) corrections with the inclusion of deformation energies [29]:

$$\Delta E^{\mathrm{Stab}} = -(E^{\mathrm{complex}} - \sum E^{\mathrm{fragment}}) - \Delta E^{\mathrm{deform}} \quad (1)$$

where E^{fragment} energies were evaluated in fixed geometry from the complex optimized structure with basis functions localized on 'ghost' atoms. $\Delta E^{\mathrm{deform}}$ (fragment) was evaluated for each ligand (base, acetic acid, and water molecules): $\Delta E^{\mathrm{deform}}(\mathrm{fragment}) = E^{\mathrm{Opt}} - E^{\mathrm{Fr}}$ as a difference between fully optimized geometry and the fixed structure taken from the complex (evaluated without additional functions of the ghost atoms). The final $\Delta E^{\mathrm{deform}}$ energy is a sum over all fragments deformation energies in the complex. The determination of Gibbs free energies is based on the microcanonical statistical ensemble. Individual contributions to partition functions were obtained from combination of the (single point) energies at B3LYP/6-31++G(d,p) level and frequency analysis performed at the B3PW91/6-31G(d) level. At this level, the calculations also served as a test that the obtained structures have the proper character of minimum (all the frequencies of normal vibration modes have positive values).

Two types of stabilization energies were considered, namely energies with and without ligand repulsion corrections [30]. In the calculation of ΔE^{Stex}, all ligands are considered as a single fragment in Eq. (1) in the form of a fixed shell (optimized position taken from complexes geometry) where only the two rhodium cations are missing. These two cations (with fixed Rh–Rh distance) are considered as the second fragment. In the evaluation of ΔE^{Stab} energies (without these corrections) every ligand is considered separately. It means that 6 separate calculations for each ligands + one calculation of dirhodium kernel were necessary for evaluation of the ΔE^{Stab} energy (besides the total energy of the whole complex) while only two calculations are required for the determination of the ΔE^{Stex} energy.

BE's were calculated according to the analogous formula without the deformation energy corrections and the partitioning of the complex for the calculation of the E^{fragment} energies is taken according to the examined bond(s).

Electronic properties (partial charges, dipole moments, MOs, and the natural population analysis (NPA)) and electrostatic potentials were determined at the level used in energy analyses. For determination of the electronic structures, the Gaussian 98 program package was used; the atomic population from NPA was obtained using the program NBO v.5.0 from Wisconsin university [31].

The starting point for the substitution reactions is the electroneutral diaqua-tetrakis(μ-acetylato)dirhodium(II,II) complex $[Rh_2(OAc)_4w_2$ (where $OAc = CH_3COO^-$ and w means aqua-ligands in axial positions)] in the singlet elec-

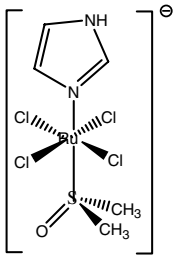

Formula 1

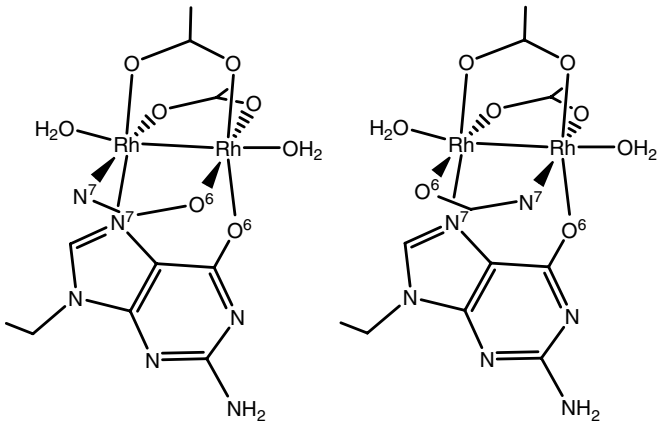

Scheme 1. HH and HT arrangement of diguanine complexes.

tronic ground state. Then, one of the acetyl groups was replaced by N1-deprotonated 9-ethylguanine or 9-ethyladenine deprotonated in N6 position. The standard [32] numbering of the DNA-bases atoms is used in this study. The deprotonation is expected to occur during metal addition [21]. Some more details on the experiments where deprotonation of N1 site of guanine was observed can also be found in Ref. [33]. In the second reaction step, the replacement of the adjacent acetyl ligand by another deprotonated base (either 9EtG or 9EtA) was simulated. In this way three head-to-head (HH) complexes $[Rh_2(OAc)_2(B_1B_2)w_2$ (B_i = 9EtG or 9EtA)] and one head-to-tail (HT) complex $[Rh_2(OAc)_2(9EtG)_2w_2]$ were examined. Head-to-head arrangement means that both guanine bases are attached with same position (e.g., N7) to the first metal atom and with the other (O6) to second metal atom as it can be see in Scheme 1.

In case of HT orientation, O6 of one guanine and N7 site of another coordinate to one metal atom. For the estimation of the base–base repulsion, the classical electrostatic interaction was estimated according to Coulomb law where atomic partial charges q_i were taken from the NPA analysis.

3. Structural parameters of the complexes

All optimized structures of dirhodium complexes can be found in Fig. 1 and the most important geometry characteristics are collected in Table 1. The intermetallic distances reflect the number and types of the bases. While the tetraacetate complex exhibits a relatively short Rh–Rh bond length (about 2.39 Å), this distance is 2.43 Å in the complex with guanine and 2.44 Å in the complex with adenine. Similarly in the two-base complexes, the diguanine structure

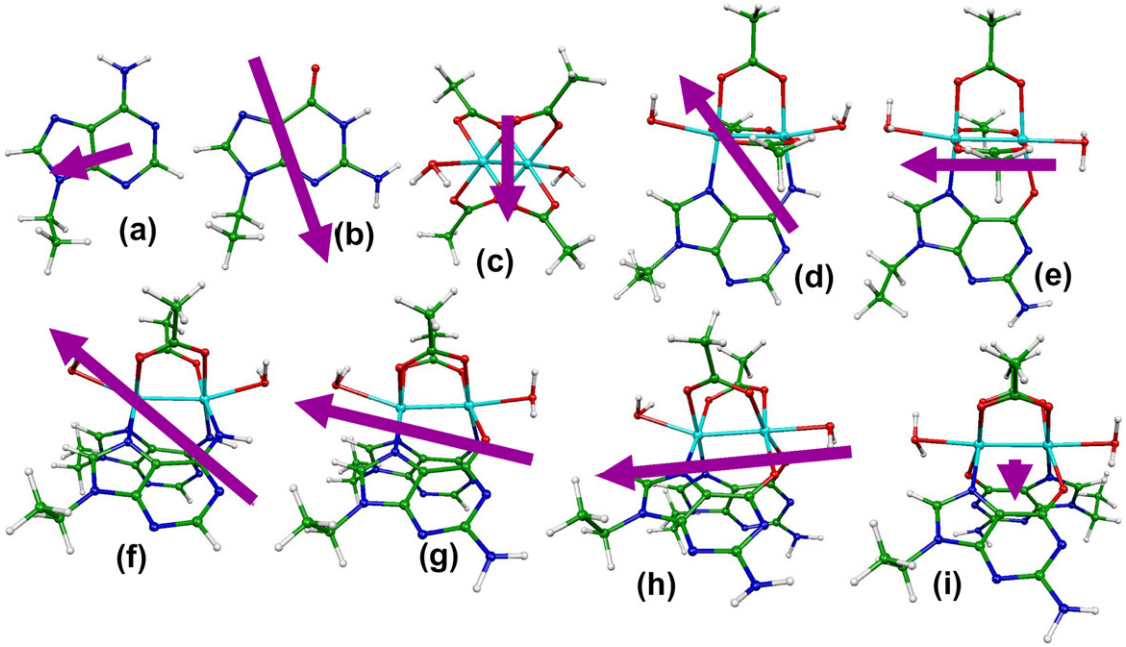

Fig. 1. Optimized structures with the orientation of dipole moments (violet arrows) of dirhodium complexes with 9Et-guanine(s) and 9Et-adenine(s): (a) isolated adenine, (b) isolated guanine, (c) tetraacetato-diaqua-dirhodium complex, (d) adenine adduct with dirhodium complex, (e) guanine adduct with dirhodium complex, (f) diadenine complex with dirhodium, (g) mixed adenine–guanine complex, (h) HH–diguanine complex, (i) HT–diguanine-diacetato-diaqua-dirhodium complex. (For interpretation of the references to colour in this figure legend, the reader is referred to the web version of this article.)

Table 1
Selected bond distances (in Å) involving in the co-ordinations of Rh(II) cations and torsion angles (in degrees) which demonstrate the distortions of dibase complexes

	(OAc)4	(OAc)3A	(OAc)3G	(OAc)2A2	(OAc)2AG[c]	(OAc)2G2	(OAc)2G2_HT
Rh–Rh	2.386	2.435	2.429	2.496	2.488	2.481	2.483
Rh–O6/Rh–N6		1.992	2.023	1.992	2.022g/1.991a	2.018	2.027
Rh–N7		2.012	2.015	2.013	2.019g/2.013a	2.017	2.014
Rh–O(OAc) 6–end	2.041	2.056[b]	2.045	2.100	2.049g/2.098a	2.05	2.054
Rh–O(OAc) 7-end	2.056[a]	2.055[b]	2.047	2.069	2.064g/2.060a	2.06	*2.054*
Rh–O(w6) 6-end	2.347	2.325	2.318	2.296	2.292	2.272	2.389
Rh–O(w7) 7-end	2.347	2.422	2.422	2.490	2.493	2.502	*2.389*
O(OAc)–Rh–Rh–O(OAc)	0.0	0.0	0.0	9.4	9.0	8.2	0.0
O(OAc)–Rh–Rh–O(OAc)	0.0	0.0	0.0	9.2	8.3	10.5	0.0
N7–Rh–Rh–X6	0.0	0.0	0.0	10.0	10.2a	11.2	0.0
N7–Rh–Rh–X6	0.0	0.0	0.0	10.3	11.8g	10.5	0.0

[a] Rh–O distances influenced by H-bonding from water in axial position.
[b] Rh–O in *cis*-positions to adenine, values of OAc in *trans*-positions are 2.092 and 2.067 Å for 6-end and 7-end, respectively.
[c] Numbers labeled with "g" and "a" mean value for guanine and adenine, respectively, and in lines Rh–O (OAc) it signs value for adjacent acetato-ligand to the given base.

displays Rh–Rh bond length ca. 2.48 Å (in both HH and HT orientations), the distance of 2.49 Å can be observed for the mixed AG complex, and 2.50 Å for the diadenine complex. The larger dinuclear bond length corresponds to the longer distance between N7 and X6 sites in DNA purine bases in comparison with the $\widehat{OO}$ distance in the acetyl group.

While the Rh–N bond is relatively insensitive to its neighborhood (1.99 Å for Rh–N6 and 2.01–2.02 Å for Rh–N7), the Rh–O distances exhibit a much larger variability. Even in the symmetrical tetraacetylatodirhodium complex, the specific orientation of water molecules causes a differentiation of the Rh–O(Ac) bonds by about 0.015 Å. The longer Rh–O bonds occur in the presence of O(Ac)···H(w) interactions despite the fact that these interactions are relatively very weak (the O···H distance is more than 2.1 Å). Due to the different base interaction sites, the difference increases up to 0.05 Å for Rh–O of acetyl ligands in *trans*-position to N6–adenine coordination. This can be explained by a strong *trans* effect of the partially deprotonated N6 amino group. The Rh–O6 distance in guanine complexes varies within 0.01 Å – the shortest dative bond is in the HH diguanine isomer (2.018 Å), while the longest bond (2.027 Å) is in the HT isomer. An interesting situation occurs in the case of the Rh–O(w) distances. They represent the longest bond distances and exhibit the widest range of fluctuations (from 2.27 to 2.50 Å). These facts point to a very weak electron pair donation from the water oxygen to the metal cation. The largest difference in Rh–O(aqua) is caused by the different bonding moiety of the N7 and O6 bonding sites in the HH diguanine complex. While at the O6 sites, the H-bondings strengthen the Rh–O dative bond, in the N7 domain the Rh–O coordination is weakened by the additional H8···O(w) interactions, which take away part of the electron density from the Rh–O(w) area.

In the case of complexes with two bases in HH orientation, some distortion of the molecular structure occurred. Here, the axis of the Rh–Rh bond displays deviation from the planes of DNA bases or acetyl-ligands. In the lower part of Table 1, the *X*–Rh–Rh–*Y* dihedral angles were collected where *X* and *Y* are either oxygens in OAc ligands or N7 and O6/N6 atoms in DNA bases. Such a distortion decreases the base–base repulsion and improves the final stabilization of the complex. Without such a distortion, the distances between the pairs of atoms of the same kind (e.g., O6···O6, with the same charge either negative or positive) are shorter than when some shift between bases occurs.

In the complexes with guanine, relatively strong H-bonds are formed between the water molecule (closer to the O6 site) and oxygen atom of guanine. Such an H-bond weakens the Rh–O6 coordination. This can be demonstrated, e.g., by areas of lower values of electrostatic potential displayed in the Fig. 2 and in Table 2.

4. Energy relations and thermodynamics

Energy analyses of the studied dirhodium complexes are summarized in Table 2. Many local minima were explored and the following analyses were performed for the lowest lying conformers. The first row contains the stabilization energies ΔE^{Stab} and, similarly to square platinum complexes [34], the stabilization energy increases with the number of DNA bases in the Rh_2 moiety by about 10–15 kcal/mol. This reflects the higher affinity of the dirhodium kernel to nitrogen atoms in correspondence with the hard–soft–acid–base (HSAB) principle [35]. The estimation of the corrected stabilization ΔE^{Stex} (where the ligand···ligand interaction is subtracted from the ΔE^{Stab} energy) gives substantially higher metal–ligand coordination energies. This is due to the fact that the electrostatic repulsion of ligands (each of them carries −1 negative charge) is not included. On the contrary to the ΔE^{Stab} energies, the ΔE^{Stex} values decrease with the number of coordinated DNA bases. An explanation follows from the fact

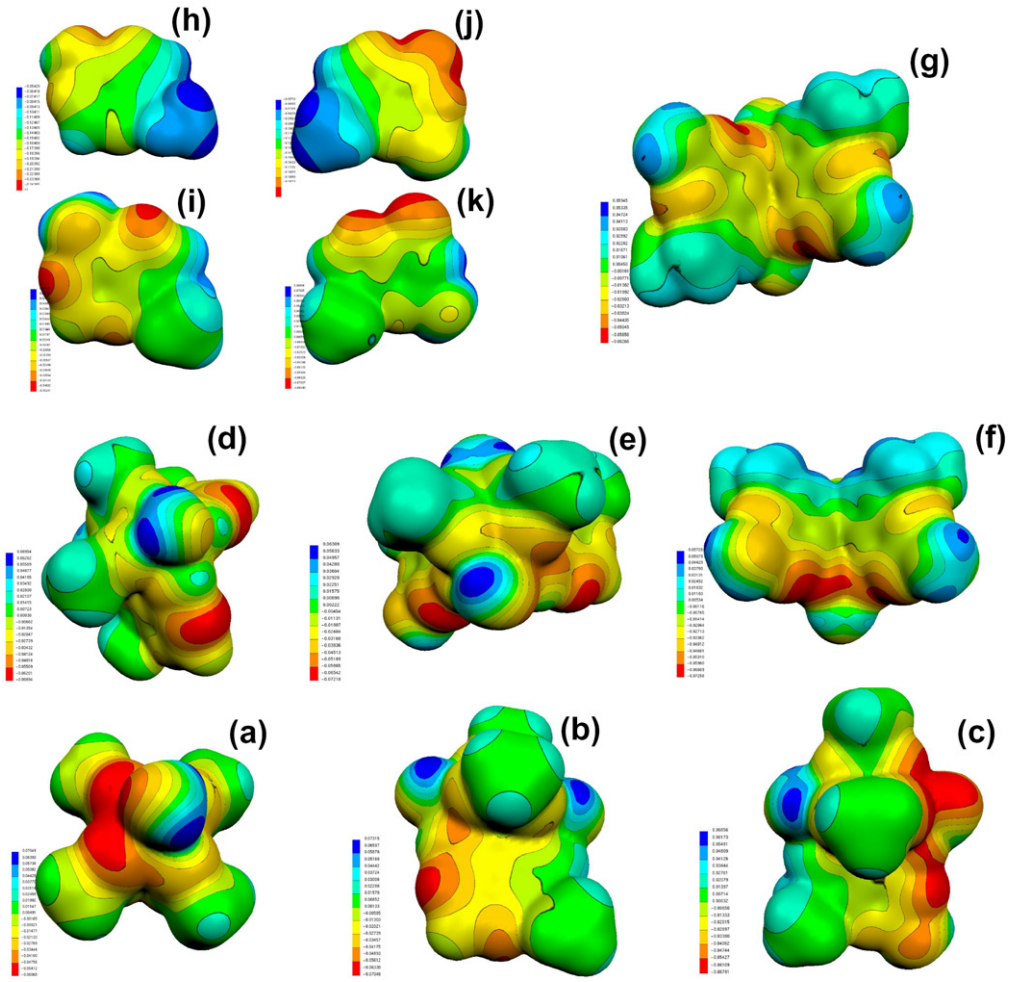

Fig. 2. Maps of electrostatic potentials for dirhodium complexes. The scaling (V_{min} and V_{max}) for the depicted structures can be found in Table 2. (a) $Rh_2OAc_4w_2$; (b) $Rh_2OAc_3Aw_2$; (c) $Rh_2OAc_3Gw_2$; (d) $Rh_2OAc_2A_2w_2$; (e) $Rh_2OAc_2AGw_2$; (f) $Rh_2OAc_2G_2w_2$; (HH) (g) $Rh_2OAc_2G_2w_2$; (HT) (h) anion A^-; (i) electroneutral 9EtAH; (j) anion G^-; (k) electroneutral 9EtGH. Dark blue areas corresponds to the most positive values, red color corresponds to the surface with negative potential.

Table 2
Stabilization and bonding energies of dirhodium complexes (in kcal/mol), extremal values of electrostatic potentials and dipole moments μ (in D)

	(OAc)4	(OAc)3A	(OAc)3G	(OAc)2A2	(OAc)2AG	(OAc)2G2	(OAc)2G2_HT
ΔE^{Stab}	1917.3	1930.1	1922.1	1941.8	1933.6	1923.8	1931.0
ΔE^{Stex}	2349.9	2334.3	2330.2	2323.1	2321.7	2317.4	2324.1
BE(B1)		191.8	186.4	182.7	187.5	177.2	183.4
BE(B2)				184.2	178.1	177.8	*183.4*
BE(OAc)		171.4[a]	173.0[a]				
BE(OAc1)	179.5	168.7[a]	172.6[a]	165.6	168.2	169.5	170.6
BE(OAc2)	176.1	170.7[a]	173.8[a]	166.2	168.5	170.2	*170.6*
BE(w6)	7.5	8.8	10.5	10.3	12.1	13.3	11.7
BE(w7)	*7.5*	8.5	8.7	9.1	9.5	9.1	*11.7*
V_{min}	−38.1	−44.2	−42.6	−43.3	−45.3	−45.5	−39.3
V_{max}	44.2	45.9	43.0	43.6	39.6	35.9	37.3
μ	3.44	6.40	5.22	9.35	8.66	9.04	0.92

$V_{min} = -53.6/-42.7$ and $V_{max} = 54.3/44.6$ kcal/mol for isolated guanine/adenine can be compared with similar calculations from Ref. [45]. Dipole moments of isolated 9Eth-adenine/guanine are 2.67/7.28 D.

[a] BE(OAc) and BE(OAc1) means *cis*-acetyl ligands towards DNA base, BE(OAc2) is *trans*-acetyl ligand.

that smaller acetyl ligands have their negative charge concentrated only on the oxygen atoms (close to rhodium cations), which causes higher interligand repulsion. In the case of larger DNA bases, the negative charge is (at least partially) smeared over several electronegative heteroatoms, which are more distant from the dirhodium kernel. Thus,

the electrostatic repulsion is substantially (by up to 30 kcal/mol) reduced. Interestingly, the total ligand repulsion energy ($\Delta E^{Stab} - E^{Stex}$) is practically the same in the both HH and HT diguanine systems. Nevertheless the base-base repulsion energy is smaller in HT orientation. The base···base repulsion energies were determined using the classical Coulomb-law formula employing NBO partial charges. In this way, it can be estimated that guanine bases in HH arrangement repel each other by about 40 kcal/mol while the repulsion of only 23 kcal/mol was obtained for the HT conformation. A partial compensation of the larger base···base repulsion in HH arrangement correlates with the distortion of the ligands in all the three HH complexes explored, as discussed in the section on complex structures. This can be compared with the HH and HT arrangements in cisplatin complexes, where ΔE^{Stab} for the HT conformer is by about 2.5 kcal/mol higher than for the HH one [36].

Table 2 further contains the coordination energies of individual ligands. Notice that in the tetraacetylatodirhodium complex, the four acetyl groups are not equivalently coordinated. A small difference (about 3 kcal/mol) is caused by asymmetrically bonded water molecules in accord with the geometry parameters discussed above. Seemingly stronger Rh–O(OAc) dative bonds occur in the case where H-bonds between H(axial aqua) and O(OAc) are formed. The explanation can be seen in the fact that the actual reduction of the Rh–O bond is compensated by the formation of relatively strong H-bonds between polarized O(OAc) and axial water. This results in a larger total BE value for those acetyl-ligands that are involved in H-bonding. In complexes with a single adenine, H-bonds between water and two acetyl-ligands are preferred leading to an increase in net Rh–O(OAc) coordination energies by 2 kcal/mol (in comparison with the third acetyl ligand, which is not involved in H-bonding). Practically no energy weakening caused by the *trans*-effect is observable in single-base complexes. It can be estimated that the reduction in the coordination energy of the visibly longer Rh–O(OAc) distance in *trans* position to the N6 site of adenine is compensated by H-bond interaction in analogy with bonding relations in the tetraacetate complex. The lower coordination energies of acetyl ligands in the adenine complexes are in comparison with the guanine complexes is due to the stronger donation competition with two nitrogen atoms (N6, N7) in adenine than with O6 and N7 sites of guanine. Also, the monotonic decrease in the acetyl-ligand binding energy with number of bases is linked to the higher affinity of both DNA bases to the dinuclear Rh kernel.

The most important characteristics are the binding energies of the DNA bases. In all studied complexes, adenine dative bonds are slightly stronger (up to 5 kcal/mol per base) in comparison with guanine bonds. This is a completely different picture than in the case of the cisplatin interaction with bases. However, it is in good accord with Pearson's HSAB principle, since the interaction of (softer) transition metals like rhodium with nitrogen atoms should be stronger than with the relatively hard oxygen atoms. Contrary to cisplatin or the recently reported "piano-stool" Ru(II) complexes [13,15,37,38], where only N7 coordination can occur, here two different sites (N7 and X6) are involved in the metal–base interaction. Thus not only the different polarizability or dipole moment can be used for the characterization of the differences between metal–base bondings [34,39–42]. The stronger interaction of adenine can be explained by the stronger Rh–N6 dative bond in comparison with the Rh–O6 bond in guanine. When the HH and HT diguanine conformers are considered, markedly higher guanine coordination energies follow from the fact that in the HT conformation the two N7 sites are not localized on the same rhodium atom and therefore the competition between these two N7 sites vanishes. This points to some kind of saturation of the electron donation to the vacant orbitals of the transition metal. We also saw this effect in some other calculations, which involved platinum [34,40], ruthenium [43], and copper [44] complexes. Also, the lower coordination energy of adenine in the diadenine complex in comparison with the mixed AG complex can be explained on the same basis. It can be guessed that HT orientation in the diadenine complex would not lead to an analogous increase in stability like in diguanine complexes due to the approximately same local softness of both N6 and N7 atoms and thus the donation to the metal atom should not increase.

The axial water coordination to the dirhodium(II) complex is very weak and resembles much more the H-bonding behavior than a dative bond. This is further supported by the fact that the lone electron pairs of water are not properly oriented towards the metal atoms due to H-bond interactions to the oxygen atoms of adjacent acetyl-ligands or O6 site of guanine. Notice that no H-bonds involve adenine. From the NBO analysis (cf. discussion of partial charges below), the less negative water oxygen is in the X6 region. This corresponds to the stronger donation of the oxygen lone electron pair to metal and correlates also with shorter Rh–O(w6) distances in the X6 region. In the case of guanine, the stronger interaction of water with the dirhodium kernel in the O6 vicinity (above 10 kcal/mol) is connected with stronger H-bonds in this region. Since the N6 positions do not interact with the axial water molecules, a smaller difference between both axial ligands exists in the diadenine case (as well as in the symmetrical HT–diguanine conformation).

Finally, reaction energies (ΔG) for the acetyl ligand replacement were determined. Two possible types of reactants (and products) were considered: (i) the interaction of electroneutral 9-ethylguanine/adenine, which led to neutral acetic acid and (ii) the interaction of 9-ethylguanine/adenine anions, where the N1/N6 position was deprotonated. In this case, an acetyl anion was the reaction product. The obtained reaction energies are collected in Table 3. From this table, it can be noticed that while the replacement of neutral guanine is a less demanding process, the N6 deprotonated form is connected with a higher energy release in the adenine case. The preference for a deproto-

Table 3
Reaction energies, enthalpies and Gibbs energies for the replacement of the acetyl ligands by DNA bases (in kcal/mol)

	$\Delta E1$	$\Delta E2$	$\Delta H2$	$\Delta G2$
$Rh–OAc_4 + B(H) \rightarrow Rh–OAc_3B + OAc(H)$				
A	−4.4	−11.0	−8.1	−11.9
AH	1.5	0.2	2.8	**−0.6**
G	5.1	−0.7	1.9	−2.3
GH	−5.0	−6.7	−4.1	**−7.8**
$Rh–B1 + B2(H) \rightarrow RhB1B2 + OAc(H)$				
A2/AA	−3.1	−9.1	−8.5	−7.2
A2H/AA	2.9	2.2	2.4	**4.1**
A2/AG	−3.2	−9.4	−8.9	−7.9
A2H/AG	2.8	1.9	2.0	**3.4**
G2/AG	6.3	0.9	1.1	1.7
G2H/AG	−3.8	−5.1	−4.9	**−3.8**
G2/GG_HH	7.7	2.2	1.8	5.1
G2H/GG_HH	−2.4	−3.7	−4.3	**−0.3**
G2/GG_HT	2.1	−4.1	−3.7	−0.4
G2H/GG_HT	−8.0	−10.1	−9.7	**−5.9**

Level $\Delta E1$ means optimization calculations, $\Delta E2$ single-point energy evaluations.

nated base correlates with the corresponding pK constants. When only the N7 bonding site was employed, the expected pK_a(N1) would be about 8.5 similarly to cisplatin d(GpG) crosslinks. In the case of μ-dirhodium complexes, pK_a(N1–guanine) is about 5.7 in the given environment [21]. Larger pK_a value can be expected for the dissociation of the N6–H bond of adenine. The formation of the N6 deprotonized adenine is substantially more demanding. Therefore, when a less stable deprotonated adenine form is considered, a more exothermic reaction course is obtained.

In the first reaction step, when one of the four acetyl ligands is replaced, the thermodynamic potential for guanine (regular N1-protonated form, which is present in real DNA chains) is by about 7 kcal/mol lower (a more exothermic course) than for adenine. Despite that the exact mechanism for the replacement reaction is not known, it can be assumed that the first interaction site will concern the N7 position of a base and in this case a stronger affinity to guanine can be expected in accord with analogous interactions with other metal complexes like cisplatin.

In the second step, only a minor ΔG preference was obtained in the second adenine replacement in the case of the dirhodium–monoguanine complex in comparison with the dirhodium–monoadenine one. For the second guanine replacement, it holds that the creation of a mixed complex is preferred to a diguanine complex. However, this assumes that the dirhodium–monoadenine complex already exists. In the case when the HT diguanine structure is formed, a larger energy release can be noticed. This point to a larger donation competition of the N7 guanine site in the HH orientation.

5. Electronic properties

An analysis of molecular orbitals was performed for the optimized structures. Orbital energies of the most important MOs are collected in Table 4. The highest eigenvalues (about −0.181 a.u.) of the HOMO occur in the adenine-containing complexes. In this way the adenine complexes show a higher affinity for nucleophilic attack (cf. also below the discussion of electrostatic potentials). Also the smallest HOMO–LUMO gap can be seen in the Rh_2OAc_3A complex (ca. 0.121 a.u.) and generally this gap is smaller in all the adenine containing complexes. In all examined complexes, a surprisingly uniform picture was discovered. The LUMO (Fig. 3h) is a δ^*_+ antibonding combination of Rh–Rh d_{+2} atomic orbitals (plus in subscript of δ is linked with d_{+2} AOs); lower eigenvalues can be observed in complexes with two DNA bases. HOMO is an orbital with a high occupation of d_0 AOs on the Rh atoms (cf. Fig. 3g). Then, usually three MOs follow with antibonding π^* and δ^*_- characters of d_{xz}, d_{yz}, and d_{xy} AOs on the Rh atoms (Fig. 3, pictures d–f). After these MOs a remarkable gap occurs (more than 0.4 eV), which is stressed in the Table 4 by (the first) horizontal line. In the next "band", σ, δ, and π bonding combinations of the metal atomic orbitals can be found (Fig. 3, pictures a–c). It is interesting that below these eigenvectors another quite distinct gap occurs (about 0.2 eV) and the other MOs follow with eigenvalues lower than −0.28 a.u.

Table 4
Eigenvalues of the most important MOs

OAc4	OAc3A	OAc3G	OAc2A2	OAc2AG	OAc2G2_hh	OAc2G2_ht
-0.052	-0.061	-0.059	-0.069	-0.067	-0.065	-0.064
-0.202	-0.182	-0.205	-0.181	-0.183	-0.202	-0.201
-0.205	-0.208	-0.207	-0.193	-0.207	-0.206	-0.206
-0.205	-0.211	-0.208	-0.218	-0.216	-0.212	-0.209
-0.248	-0.212	-0.210	-0.219	-0.217	-0.214	-0.212
-0.250	-0.240	-0.236	-0.222	-0.219	-0.216	-0.212
-0.261	-0.247	-0.248	-0.241	-0.239	-0.234	-0.231
-0.262	-0.253	-0.251	-0.244	-0.241	-0.241	-0.243
-0.290	-0.261	-0.257	-0.246	-0.245	-0.246	-0.249
-0.299	-0.262	-0.268	-0.259	-0.252	-0.249	-0.251
-0.300	-0.277	-0.270	-0.261	-0.260	-0.250	-0.251
-0.313	-0.283	-0.285	-0.270	-0.266	-0.263	-0.264
-0.314	-0.284	-0.296	-0.273	-0.272	-0.265	-0.265
-0.316	-0.299	-0.298	-0.277	-0.275	-0.275	-0.273
-0.317	-0.302	-0.305	-0.283	-0.285	-0.285	-0.282
-0.318	-0.308	-0.307	-0.287	-0.286	-0.290	-0.286

The sections divided by vertical lines point to 'shell electronic structures' and they should stress relatively larger gap between subsequent eigenvalues between the corresponding MOs.

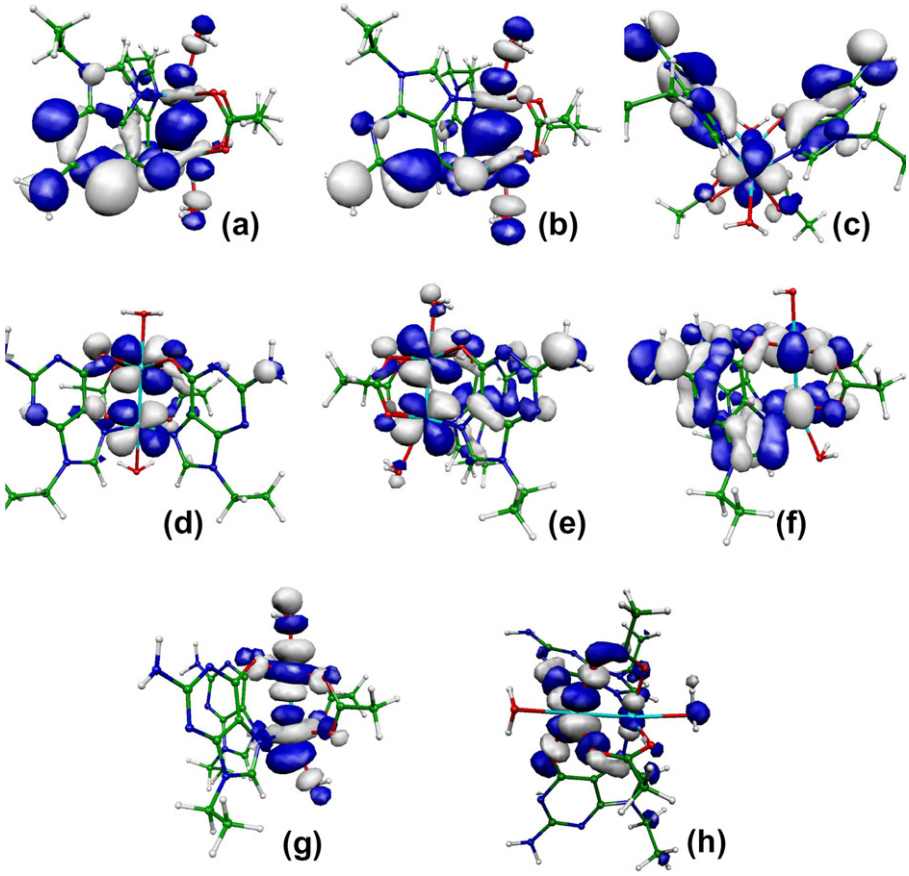

Fig. 3. Molecular orbitals of the $Rh_2OAc_2G_2w_2$ (HH) complex: (a) 144th and (b) 145th MOs with σ-bonding character of the Rh–Rh atoms; (c) 146th MO with δ-bonding character; (d) 147th and (e) 148th MOs represent π-antibonding character; (f) 149th MO has δ and (g) HOMO (152nd MO) has σ-antibonding character; (h) LUMO with δ-antibonding character on the Rh–Rh subpart. (For interpretation of the references to colour in this figure legend, the reader is referred to the web version of this article.)

The NPA partial charges of the DFT optimized structures were examined and the determined charges of chosen atoms are summarized in Table 5. In the tetraacetate complex, a symmetrical electron density distribution occurs between both Rh atoms. In single-base and HH complexes, a difference between the Rh atoms is enforced by the different bonding character of the N7 and X6 coordination sites of the bases. The larger positive partial charge of the Rh atom is linked with a smaller donation from the ligands. In Table 5 it can be observed that the highest δ(Rh) is connected with O6 guanine coordination ($\delta = 0.97$ in the diguanine complex). Simultaneously, the lowest partial charge occurs on the neighbouring Rh atom of the same complex, which is coordinated to the N7 site ($\delta = 0.67$). The different charge population of both Rh atoms corresponds with the coefficients of the natural bond orbital (NBO) of the Rh–Rh bond. This orbital contains a higher contribution of the Rh atom, which is coordinated to the N7 atom(s). The largest Rh partial charge disproportion (58%Rh(N7) vs. 42%Rh(O6)) was found in the HH diguanine complex.

The consequences of the different base interaction sites (N7 and X6) can be also noticed in the electron density localized on the water molecules. A small positive charge prevails on these molecules in all examined complexes even without any DNA base. This charge transfer can be also observed in the maps of electrostatic potentials where positive blue areas dominate in the Rh-aqua ligands regions (cf. Fig. 2). The difference of the electron density on both water molecules is about 0.06e in the diguanine complex. As to partial charges on atoms of the bases, the pronounced polarization effects are remarkable under base coordination to the dirhodium complex. The most pronounced deviations from the isolated base were found in the partial charges of the C8 (up to 0.08e), H8, N1, and N3 sites (0.06e) in guanine as well as in adenine complexes. These pronounced polarizations speak out about substantial changes in electron densities due to the formation of Rh_2 adducts.

Analogous changes are also visible from the electrostatic maps depicted in Fig. 2. The values of minima and maxima of the individual potentials on the isodensity surface ($\rho = 0.001$ e/Å^3) are compiled in the lower section of Table 2. It can be seen that always the N7 moiety is connected with a relatively large positive potential (H8 and H(w)) and the N1 proximity with a negative potential. This corresponds to the inhomogeneity of charge distribution on the Rh atoms discussed above. The orientations of negative and positive areas are confirmed by the dipole moments summarized in the last line of Table 2 and Fig. 1. The

Table 5
NPA partial charges on selected atoms of the dirhodium complexes (in e)

OAc4		OAc3A		OAc3G		OAc2A2		OAc2AG		OAc2G2_HH		OAc2G2_HT	
Rh	0.884	Rh6	0.843	Rh6	0.931	Rh6	0.801	Rh6	0.886	Rh6	0.969	Rh	0.828
Rh	0.884	Rh7	0.795	Rh7	0.781	Rh7	0.697	Rh7	0.687	Rh7	0.671	Rh	0.828
O	−0.674	Oac6i	−0.662	Oac6i	−0.640	Oac6	−0.685	Oac6	−0.684	Oac6	−0.638	Oac6	−0.683
O	−0.677	Oac7i	−0.686	Oac7i	−0.691	Oac7	−0.712	Oac7	−0.708	Oac7	−0.706	Oac6′	−0.683
O	−0.653	Oac6o	−0.648	Oaco6	−0.667	Oac6′	−0.692	Oac6′	−0.633	Oac7′	−0.711	Oac7	−0.652
O	−0.652	Oac7o	−0.661	Oaco7	−0.659	Oac7′	−0.705	Oac7′	−0.712	Oac6′	−0.640	Oac7′	−0.652
O	−0.674	Oac6t	−0.693	Oac7t	−0.697	N6	−0.719	O6	−0.690	O6	−0.679	O6	−0.710
O	−0.677	Oac7t	−0.700	Oac6t	−0.644	N7	−0.442	N7	−0.438	N7	−0.438	N7	−0.441
O	−0.653	N6	−0.732	O6	−0.695	N6′	−0.722	N6′	−0.719	O6’	−0.681	O6’	−0.710
O	−0.652	N7	−0.446	N7	−0.445	N7′	−0.439	N7′	−0.443	N7’	−0.443	N7’	−0.441
Ow	−0.954	Ow6	−0.952	Ow6	−0.954	Ow6	−0.947	Ow6	−0.951	Ow6	−0.942	O	−0.983
Ow	−0.954	Ow7	−0.974	Ow7	−0.977	Ow7	−0.988	Ow7	−0.989	Ow7	−0.990	O	−0.983
H	0.520	Hw6	0.525	Hw6	0.533	Hw6	0.529	Hw6	0.536	Hw6	0.530	H	0.535
H	0.519	Hw6	0.524	Hw6	0.515	Hw6	0.529	Hw6	0.521	Hw6	0.529	H	0.535
H	0.519	Hw7	0.526	Hw7	0.524	Hw7	0.523	Hw7	0.524	Hw7	0.523	H	0.522
H	0.520	Hw7	0.523	Hw7	0.525	Hw7	0.524	Hw7	0.524	Hw7	0.523	H	0.522

dipole moment occurring in the diadenine complex is slightly larger than in the diguanine complex. However, the orientation and size of the dipole moment is influenced by the orientation of the axial water molecules, which can partially mask or modify the effects of the electron redistribution of the bases. The dipole moments of the isolated neutral bases are included for the demonstration of the extent of the electron density redistribution.

6. Conclusions

In this study, the diaqua-tetrakis(μ-acetylato)dirhodium(II,II) complexes were explored. The replacement of the acetyl-ligand by a DNA base was simulated in two steps. Both head-to-head and head-to-tail diguanine complexes were considered. Only HH diadenine and mixed adenine–guanine complexes were examined.

The optimization of the complexes was performed at the DFT level employing the B3PW91 functional and 6-31G* basis set. For the Rh description, Stuttgart–Dresden MWB-28 pseudopotentials were used. The complexes were described in singlet electronic ground states. The energy and electron density analyses were determined at the B3LYP/6-31++G(d,p) level.

Higher stabilization as well as bonding energies was found for the adenine coordination in comparison with guanine (by about 5 kcal/mol per base). Since adenine interacts through two nitrogen atoms (N6 and N7) and guanine through O6 and N7 sites, this result matches Pearson's HSAB principle and is also supported by the NPA analysis.

However, despite the larger stabilization energies of adenine complexes, the thermodynamic description of the replacement reaction favors neutral guanine. The more exothermic reaction course (by about 7 kcal/mol) is connected with an easier proton transfer from the N1 position of neutral guanine to acetic acid anion in comparison with the N6 site of adenine. This is also in good accord with the experimentally found decrease of pK_a(N1–guanine). While the value of 9.5 was determined for isolated guanine, $pK_a = 5.7$ was estimated for the dirhodium–guanine complex in study [21].

It was found that the axial aqua-ligands are bonded very weakly, up to 13 kcal/mol. Such an amount of energy corresponds to an H-bond rather than a dative bond especially in highly polarized complexes like these.

According to the higher-lying HOMO and a smaller HOMO–LUMO gap of the adenine complexes, we can expect their higher reactivity.

Electrostatic potential maps were drawn for the complexes showing a large negative potential in the N1–X6 area and a positive potential in the moiety of the N7 coordination for all the complexes with DNA base(s).

Acknowledgements

The study was supported by NSF-MŠMT Grant No. 1P05ME784, GA-AV IAA400550701, and MSM 0021620835. The authors thank the Meta-Centers in Prague (Charles University and Czech Technical University), Brno (Masaryk University), Pilsen (University of West Bohemia), and Mississippi Center for Supercomputing Research for their generous support by providing the computational resources.

References

[1] B. Rosenberg, L. Van Camp, J.L. Trosko, V.H. Mansour, Nature 222 (1969) 385–391.
[2] L.Y. Kuo, A.H. Liu, T.J. Marks, in: A.S.H. Sigel (Ed.), Met. Ions Biol. Syst., Marcel Dekker, Inc., New York, Basel, Hong Kong, 1995, pp. 53–85.
[3] F. Caruso, M. Rossi, Mini-Rev. Med. Chem. 4 (2004) 49–60.
[4] J.B. Waern, C.T. Dillon, M.M. Harding, J. Med. Chem. 48 (2005) 2093–2099.
[5] R. Meyer, S. Brink, C.E.J. van Rensburg, G.K. Joone, H. Gorls, S. Lotz, J. Organomet. Chem. 690 (2005) 117–125.
[6] B.M. zu Berstenhorst, G. Erker, G. Kehr, J.C. Wasilke, J. Muller, H. Redlich, J. Pyplo-Schnieders, Eur. J. Inorg. Chem. (2005) 92–99.
[7] R.K. Narla, C.L. Chen, Y.H. Dong, F.M. Uckun, Clin. Cancer Res. 7 (2001) 2124–2133.

[8] A. Anagnostopoulou, E. Moldrheim, N. Katsaros, E. Sletten, J. Biol. Inorg. Chem. 1999 (1999) 199–208.
[9] M. Eriksson, M. Leijon, C. Hiort, B. Norden, A. Graeslund, Biochemistry 33 (1994) 5031–5040.
[10] A. Kueng, T. Pieper, R. Wissiack, E. Rosenberg, B.K. Keppler, J. Biol. Inorg. Chem. 6 (2001) 292–299.
[11] G. Sava, A. Bergarno, Int. J. Oncol. 17 (2000) 353–365.
[12] R. Aird, J. Cummings, A. Ritchie, M. Muir, R. Morris, H. Chen, P. Sadler, D. Jodrell, Br. J. Cancer 86 (2002) 1652–1657.
[13] H. Chen, J.A. Parkinson, S. Parsons, R.A. Coxal, R.O. Gould, P. Sadler, J. Am. Chem. Soc. 124 (2002) 3064–3082.
[14] R.E. Morris, R. Aird, P.D. Murdoch, H. Chen, J. Cummings, N.D. Hughes, S. Parson, A. Parkin, G. Boyd, P. Sadler, D. Jodrell, J. Med. Chem. 44 (2001) 3616–3621.
[15] O. Novakova, H. Chen, O. Vrana, A. Rodger, P.J. Sadler, V. Brabec, Biochemistry 42 (2003) 11544–11554.
[16] H.T. Chifotides, K.R. Dunbar, J.H. Matonic, N. Katsaros, Inorg. Chem. 31 (1992) 4628–4634.
[17] R. Cini, G. Giorgi, L. Pasquini, Inorg. Chim. Acta 196 (1992) 7–18.
[18] J.R. Rubin, T.P. Haromy, M. Sundaralingam, Acta Crystallogr. Sect. C-Cryst. Struct. Commun. 47 (1991) 1712–1714.
[19] D.M.L. Goodgame, C.A. Omahoney, C.J. Page, D.J. Williams, Inorg. Chim. Acta 175 (1990) 141–147.
[20] N. Katsaros, A. Anagnostopoulou, Crit. Rev. Oncol. Hematol. 42 (2002) 297–308.
[21] H.T. Chifotides, K.M. Koshlap, L.M. Perez, K.R. Dunbar, J. Am. Chem. Soc. 125 (2003) 10703–10713.
[22] H.T. Chifotides, K.M. Koshlap, L.M. Perez, K.R. Dunbar, J. Am. Chem. Soc. 125 (2003) 10714–10724.
[23] H.T. Chifotides, J.M. Koomen, M.J. Kang, S.E. Tichy, K.R. Dunbar, D.H. Russell, Inorg. Chem. 43 (2004) 6177–6187.
[24] H.T. Chifotides, P.K.L. Fu, K.R. Dunbar, C. Turro, Inorg. Chem. 43 (2004) 1175–1183.
[25] H.T. Chifotides, K.R. Dunbar, Acc. Chem. Res. 38 (2005) 146–156.
[26] D. Andrae, U. Haussermann, M. Dolg, H. Stoll, H. Preuss, Theor. Chim. Acta 77 (1990) 123–141.
[27] S. Huzinaga, B. Miguel, Chem. Phys. Lett. 175 (1990) 289.
[28] S. Huzinaga, M. Klobukowski, Chem. Phys. Lett. 212 (1993) 260–264.
[29] S.F. Boys, F. Bernardi, Mol. Phys. 19 (1970) 553–566.
[30] J.V. Burda, M. Pavelka, M. Šimánek, J. Mol. Struct. THEOCHEM 683 (2004) 183–193.
[31] F. Weinhold, University of Wisconsin, Madison, Wisconsin 53706, Wisconsin (2001).
[32] W. Saenger, Principles of Nucleic Acid Structure, Springer-Verlag, New York, 1983, pp. 556.
[33] K.R. Dunbar, J.H. Matonic, V.P. Saharan, C.A. Crawford, G. Christou, J. Am. Chem. Soc. 116 (1994) 2201–2202.
[34] J.V. Burda, J. Leszczynski, Inorg. Chem. 42 (2003) 7162–7172.
[35] R.G. Parr, R.G. Pearson, J. Am. Chem. Soc. 105 (1983) 7512.
[36] M. Pavelka, J.V. Burda, Chem. Phys. 312 (2005) 193–204.
[37] J.-G. Liu, B.-H. Ye, Q.-L. Zhang, X.-H. Zou, Q.-X. Zhen, X. Tian, L.-N. Ji, J. Biol. Inorg. Chem. 5 (2000) 119–128.
[38] F. Wang, H.M. Chen, S. Parsons, L.D.H. Oswald, J.E. Davidson, P.J. Sadler, Chem. Eur. J. 9 (2003) 5810–5820.
[39] M.H. Baik, R.A. Friesner, S.J. Lippard, J. Am. Chem. Soc. 125 (2003) 14082–14092.
[40] M. Zeizinger, J.V. Burda, J. Leszczynski, Phys. Chem. Chem. Phys. 6 (2004) 3585–3590.
[41] P. Carloni, M. Sprik, W. Andreoni, J. Phys. Chem. B 104 (2000) 823–835.
[42] K. Spiegel, U. Rothlisberger, P. Carloni, J. Phys. Chem. B 108 (2004) 2699–2707.
[43] Z. Futera, J. Klenko, J.E. Sponer, J. Sponer, J.V. Burda, J. Phys. Chem, submitted for publication.
[44] M. Pavelka, J.V. Burda, J. Mol. Model. 13 (2006) 367–379.
[45] J.S. Murray, Z. Peralta-Inga, P. Politzer, K. Ekanayake, P. Lebreton, Int. J. Quant. Chem. 83 (2001) 245–254.